

Point containment algorithms for constructive solid geometry with unbounded primitives

Paul K. Romano^{a,*}, Patrick A. Myers^b, Seth R. Johnson^c, Aljaž Kolšek^d, Patrick C. Shriwise^a

^aArgonne National Laboratory, 9700 S. Cass Ave, Lemont, IL 60439, United States

^bUniversity of Michigan, Ann Arbor, MI 48103, United States

^cOak Ridge National Laboratory, Oak Ridge, TN 37830, United States

^dUniversidad Nacional de Educación a Distancia, Madrid, Spain

Abstract

We present several algorithms for evaluating point containment in constructive solid geometry (CSG) trees with unbounded primitives. Three algorithms are presented based on postfix, prefix, and infix notations of the CSG binary expression tree. We show that prefix and infix notations enable short-circuiting logic, which reduces the number of primitives that must be checked during point containment. To evaluate the performance of the algorithms, each algorithm was implemented in the OpenMC Monte Carlo particle transport code, which relies on CSG to represent solid bodies through which subatomic particles travel. Two sets of tests were carried out. First, the execution time to generate a high-resolution rasterized image of a 2D slice of a detailed CSG model of the ITER tokamak was measured. Use of both prefix and infix notations offered significant speedup over the postfix notation that has traditionally been used in particle transport codes, with infix resulting in a 6× reduction in execution time relative to postfix. We then measured the execution time of neutron transport simulations of the same ITER model using each of the algorithms. The results and performance improvements reveal the same trends as for the rasterization test, with a 4.59× overall speedup using the infix notation relative to the original postfix notation in OpenMC.

Keywords: Constructive solid geometry, point containment, particle transport, Monte Carlo

1. Introduction

Constructive solid geometry (CSG) is a technique for representing rigid solids using Boolean set operations applied to simple geometric primitives [1–3]. In CSG, a solid is represented as an ordered, binary tree where the non-leaf nodes are Boolean set operators (union, intersection, difference) and the leaf nodes represent geometric primitives. An example of such a CSG tree is illustrated in Fig. 1. CSG representations can be based on bounded primitives (cuboids, spheres, cylinders, cones, etc.) or unbounded primitives using general half-spaces.

CSG has applications in geometric modeling, computer-aided design, computer graphics, computational science, and other areas where accurate spatial modeling is required [1, 2, 4]. In particular, CSG is widely used for geometric modeling in Monte Carlo (MC) particle transport simulations through codes such as OpenMC [5], MCNP [6], Shift [7], FLUKA [8], and Serpent [9]. MC particle transport itself has applications across a wide range of scientific domains, such as nuclear reactor design, radiation shielding, medical physics, high-energy experimental physics, and fusion energy.

Most MC particle transport codes—including OpenMC, which was used for the present study—use a CSG representation based on unbounded primitives defined by inequalities of implicit surfaces. An implicit surface is a surface in Euclidean space defined by an equation $f(\mathbf{r}) = 0$. By convention, the inside of the surface is defined as

*Corresponding author. Tel.: +1 630 252 6779.

Email addresses: promano@anl.gov (Paul K. Romano), myerspat@umich.edu (Patrick A. Myers), johnsonsr@ornl.gov (Seth R. Johnson), akolšek@ind.uned.es (Aljaž Kolšek), pshriwise@anl.gov (Patrick C. Shriwise)

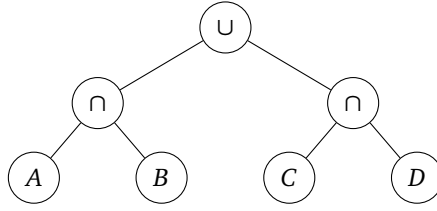


Figure 1: A CSG binary expression tree constructed with primitives (A , B , C , and D) and set intersection (\cap) and union (\cup) operators.

the set of points for which $f(\mathbf{r}) < 0$ (the negative half-space) and the outside of the surface is defined by $f(\mathbf{r}) > 0$ (the positive half-space). Thus, the leaf nodes in the CSG tree are implicit surface inequalities. Surface inequalities are then combined with Boolean set operations to create more complex solids. MC particle transport codes are typically limited to primitives based on algebraic surfaces (planes, quadrics, and sometimes torii); nearly all allow the use of set intersection and union operators, while some also provide set difference or complement operators.

Although the overall runtime of a MC particle transport simulation is distributed across many different operations, the time spent on geometric operations can be significant for large, geometrically complex models. One important geometric operation is *point containment*—given a point \mathbf{r} in space, determine whether it is contained within a particular solid. In MC particle transport simulations, this operation is used extensively for determining a particle’s location as it traverses through the geometry. In this work, we explore several algorithms for evaluating point containment in CSG trees with unbounded primitives with a goal of ultimately minimizing the execution time of MC particle transport simulations.

1.1. Point Containment

Evaluating point containment for a single unbounded primitive based on an implicit surface is straightforward. First, the implicit surface equation is evaluated at the point, $f(\mathbf{r})$, and the sign of the result is compared against the specified sign of the primitive in the CSG expression. If the sign matches, the point is contained within the primitive. Extending this to a general solid defined by a CSG tree, we can evaluate point containment by first checking point containment for all primitives, yielding a binary expression tree with Boolean leaf nodes, i.e., a Boolean expression. Evaluating this Boolean expression indicates whether the point is contained.

While evaluating point containment using a CSG tree is straightforward in principle, an important question concerning implementation remains: how should the CSG tree be represented in memory? In all the algorithms we explore here, the CSG tree is flattened into a one-dimensional data structure to improve locality of reference and minimize memory use. With a flattened data structure, the tree can be represented using either an infix, postfix, or prefix notation. Taking the CSG tree from Fig. 1 as an example, the three notations are as follows:

- Infix: $(A \cap B) \cup (C \cap D)$
- Postfix: $AB \cap CD \cap \cup$
- Prefix: $\cup \cap AB \cap CD$

While infix notation is commonly used in written language, postfix and prefix notations have the advantage of 1) being easily parsed by a computer, 2) simplifying traversal of the tree, and 3) not requiring parentheses to enforce precedence of operators.

In addition to the question of which notation is to be preferred for representing a CSG tree, a related question is whether it is possible to take advantage of short-circuiting evaluation for point containment queries, also sometimes referred to as “early-out” [10]. That is, when an intersection operator is encountered in the binary expression tree, if the first operand is found to be false it is not necessary to evaluate the second operand at all. Similarly with a union operator, the first operand evaluating to true obviates the need to evaluate the second operand. When implicit surface inequalities are used as primitives in the CSG tree, evaluating the operand is equivalent to evaluating an implicit surface function $f(\mathbf{r})$, which may bear a non-trivial cost. Thus, any notation that enables the use of short-circuit evaluation can help minimize the number of function evaluations.

For a given notation, evaluating the CSG binary expression may also require the use of a stack to manage the intermediate results of point containment on the given primitives. For postfix notation, several methods have been discussed in the literature, including bit-sequential and bit-parallel methods [10].

To our knowledge, there are no existing works in the literature discussing the use of infix, postfix, and prefix notation for representing CSG trees as used in MC particle transport codes. Based on our own survey of several popular codes, we have found that the OpenMC code through version 0.13.1 [11], Serpent, and Shift rely on a postfix notation for storing CSG trees, whereas MCNP relies on an infix notation. We are not aware of any codes that rely on prefix notation for storing CSG trees. Additionally, none of the codes surveyed use short-circuit evaluation for point containment queries as far as we are aware¹.

1.2. Summary of Contributions

The first contribution of this work is to explicitly sketch out algorithms for evaluating point containment on CSG trees using postfix notation (and postorder traversal) as well as algorithms for evaluation using infix and prefix notations. To our knowledge, no such descriptions for infix and prefix notations have been described in the existing literature. As will be shown, both infix and prefix notations enable the use of short-circuit evaluation; our second contribution is—as part of the algorithm descriptions—to demonstrate how short-circuit evaluation can be implemented when using infix or prefix notation.

For postfix and prefix notations, postorder and preorder traversal of the CSG tree require that a stack be maintained: a stack of Boolean values for postfix notation and a stack of operators for prefix notation. We discuss several strategies for minimizing the memory footprint of data structures for managing the stack and the associated computational expense of managing the stack.

The algorithm descriptions themselves are useful for understanding *how* point containment queries can be performed using various notations, but they do not by themselves provide any hard evidence why one or the other should be preferred. To study the performance of these algorithms, we have implemented all of them in the OpenMC particle transport code and performed simulations of the ITER fusion experiment, relying on an extremely detailed CSG model called E-lite [12]. These simulations demonstrate that, for problems that involve complex CSG trees, both prefix and infix notations offer substantial performance improvement by enabling short-circuit evaluation. For postfix and prefix notation, we also study how the choice of a stack data structure impacts performance.

1.3. Outline of Paper

Section 2 describes the algorithms for CSG point containment queries based on the three expression notations: postfix, prefix, and infix. It also describes data structures for managing operand/operator stacks. Section 3 describes performance results of the various algorithms as implemented in MC particle transport simulations based on the ITER experiment. Finally, Section 4 provides overall conclusions based on the results and describes the limits of the present study.

2. Methodology

2.1. Postfix Evaluation

As mentioned before, many MC particle transport codes rely on postfix notation to perform evaluation, owing to the ease by which it enables one to perform a postorder traversal (scanning the expression left to right). Most often, the user input for CSG solids in MC particle transport codes is provided using infix notation, which is then converted into a postfix notation using Dijkstra’s shunting yard algorithm [13]. The postfix notation, T , is stored in memory as a flattened array. While there are many possible approaches for representing the notation in memory, we outline the approach taken in OpenMC, which we believe to be representative of other MC particle transport codes as well. Binary CSG expression trees in OpenMC have an input representation based on the following

¹As discussed further in Section 3, some codes—including OpenMC—do implement short-circuit evaluation for CSG expressions involving only set intersection operators. However, to our knowledge none use short-circuit evaluation for *all* expressions.

conventions. First, implicit surfaces are referenced through a unique, positive integer. Implicit surface inequalities are represented by referring to the associated unique, positive integer identifying the implicit surface along with the unary positive and negative operators, which refer to the negative and positive half-spaces of the implicit surface, respectively. Thus, given two implicit surfaces identified by the integers 1 and 2, the expression “ $-1 \cap -2$ ” would represent the intersection of their negative half-spaces and “ $-1 \cup -2$ ” would represent the union of their negative half-spaces. With these conventions in mind, Fig. 2 shows an example of how the postfix notation for an expression would be represented in memory. It suffices to store each element of the array as a signed 32-bit integer. The largest integer values (e.g., $2^{31} - 1$) are reserved for operators.

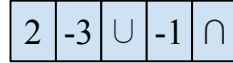


Figure 2: Memory representation (left-to-right) of the postfix notation for the expression “ $-1 \cap (+2 \cup -3)$ ”.

Algorithm 1 outlines the procedure for evaluating point containment based on an expression represented using postfix notation. This procedure is effectively performing a depth-first traversal of the original binary expression tree. Each time a primitive is encountered, the EVALUATE function, outlined in Algorithm 2, is called. Anytime a set intersection operator appears in the original binary expression tree, a logical AND operator is used on the results of the EVALUATE function, which returns a Boolean value. Similarly, a logical OR operator is used in place of the set union operator. This algorithm requires a full traversal of the expression because every evaluation of an operator requires that its operands (the implicit surface inequalities) be evaluated first. Additionally, a stack of Boolean values (evaluated operands) is necessary to keep track of the results of evaluating the primitives.

Algorithm 1 Postfix evaluation algorithm for point containment.

Require: $T \equiv$ CSG expression in postfix notation

Require: $\mathbf{r} \equiv$ point in Euclidean space

```

function CONTAINSPSTFIX( $T, \mathbf{r}$ )
   $S \equiv$  empty stack for Boolean values
  for  $i \leftarrow 1, \text{SIZE}(T)$  do
     $x \leftarrow T[i]$  ▷ Get next node
    if  $x$  is a primitive then
       $b \leftarrow \text{EVALUATE}(x, \mathbf{r})$ 
      PUSH( $S, b$ ) ▷ Store primitive containment
    else
       $b_1 \leftarrow \text{POP}(S)$  ▷ Pop two operands
       $b_2 \leftarrow \text{POP}(S)$ 
      if  $x$  is  $\cup$  then
        PUSH( $S, b_1 \vee b_2$ ) ▷ Apply logical OR
      else if  $x$  is  $\cap$  then
        PUSH( $S, b_1 \wedge b_2$ ) ▷ Apply logical AND
      end if
    end if
  end for
  return POP( $S$ ) ▷ Return top of stack
end function

```

Also note that Algorithm 1 assumes the expression only contains set union and intersection operators. Set difference and complement operators can be removed through the use of De Morgan’s laws prior to application of this procedure.

Algorithm 2 Evaluating an implicit surface inequality.

Require: $x \equiv$ node representing the implicit surface inequality $f(\mathbf{r}) > 0$ or $f(\mathbf{r}) < 0$. Let $x.\text{sign}$ be 1 when $f(\mathbf{r})$ is greater than zero and -1 when it is less.

Require: $\mathbf{r} \equiv$ point in Euclidean space

```
function EVALUATE( $x, \mathbf{r}$ )  
   $f_x \leftarrow$  function  $f(\mathbf{r})$  associated with node  $x$   
   $\phi \leftarrow f_x(\mathbf{r})$   
  return  $\text{sign}(\phi) = x.\text{sign}$   
end function
```

2.2. Prefix Evaluation

While prefix evaluation has not been previously used on binary expression trees for CSG point containment operations to our knowledge, it has an advantage over postfix evaluation in that it enables the use of short-circuiting logic and would thus avoid unnecessary evaluation of implicit surface inequalities. After a CSG expression has been converted to a postfix notation using the shunting yard algorithm, obtaining the prefix notation is as simple as reversing the postfix notation; an example prefix notation is shown in Fig. 3. Evaluation of the prefix notation then proceeds as in Algorithm 3. In this algorithm, *set operators* are pushed onto an operator stack rather than Boolean values as in postfix evaluation. By the time the second operand of a set operator is encountered, the first operand has already been evaluated, which makes it straightforward to short circuit. The algorithm for short circuiting is shown in Algorithm 4 and relies on counting the number of operators and primitives encountered. As before, Algorithm 3 assumes that only set union and intersection operators are used; other operators are assumed to have been eliminated via De Morgan’s laws.



Figure 3: Memory representation (left-to-right) of the prefix notation for the expression “ $-1 \cap (+2 \cup -3)$ ”.

2.3. Stack Memory Management

Both postfix (Algorithm 1) and prefix (Algorithm 3) evaluation algorithms require that a stack of objects be maintained. A stack data structure in C++ is typically managed through the `std::vector` class from the Standard Template Library (STL), which encapsulates a dynamically sized array. As the size of the stack grows, memory may be dynamically allocated, which is undesirable for a number of reasons. First, point containment queries in a MC particle transport simulation occur from multiple threads; because dynamic memory allocation may utilize mutual exclusion locks to ensure thread-safety, it can significantly degrade threaded performance. Second, on some compute architectures, such as GPUs, dynamic memory allocation may not be possible at all during the execution of a kernel. Here, we present techniques for minimizing memory requirements of the stack data structures utilized in the postfix and prefix evaluation algorithms such that dynamic memory allocation can be almost entirely avoided.

For postfix evaluation, a stack of Boolean values must be maintained. While the STL has a specialization of `std::vector` for the `bool` datatype that is nominally space-efficient, the actual behavior is implementation-defined and complicated by the fact that the `bool` datatype in C++ has a size of at least 1 byte (rather than 1 bit). Consequently, the implementation of `std::vector<bool>` often requires 8 bits per Boolean value. By avoiding the `std::vector` altogether, it is possible to achieve true bit-packing whereby each Boolean value is stored using a single bit. With a data structure containing a single 32-bit unsigned integer that stores the bit-packed Boolean values, one can carry out Algorithm 1 with as many as 32 Boolean values on the stack at any given point. Efficient

Algorithm 3 Prefix evaluation algorithm with short circuiting

Require: $T \equiv$ CSG expression in prefix notation**Require:** $r \equiv$ point in Euclidean space**function** CONTAINSPREFIX(T, r) $S \equiv$ empty stack for operators $b \leftarrow$ FALSE

▷ Boolean value to be returned

 $i \leftarrow 1$ ▷ Index in T **while** $i < \text{SIZE}(T)$ **do** $x \leftarrow T[i]$

▷ Get next node

if x is a primitive **then** $b \leftarrow \text{EVALUATE}(x, r)$ **while** $\text{SIZE}(S) > 0$ **do** $y \leftarrow \text{POP}(S)$

▷ Get node from stack

if y is \cup **and** $b = \text{TRUE}$ **then** $\text{SHORTCIRCUIT}(T, i)$ **else if** y is \cap **and** $b = \text{FALSE}$ **then** $\text{SHORTCIRCUIT}(T, i)$ **else****break**▷ Status value is b **end if****end while****else** $\text{PUSH}(S, x)$

▷ Store operator on stack

end if $i \leftarrow i + 1$ **end while****return** b **end function**

Algorithm 4 Skip part of prefix expression for short-circuiting.

Require: $T \equiv$ CSG expression in prefix notation**Require:** $i \equiv$ Index in T **function** SHORTCIRCUIT(T, i) $N_{\text{operator}} \leftarrow 0$

▷ Number of operators

 $N_{\text{primitive}} \leftarrow 0$

▷ Number of primitives

while $N_{\text{primitive}} \neq N_{\text{operator}} + 1$ **do** $i \leftarrow i + 1$ $x \leftarrow T[i]$

▷ Get next node

if x is a primitive **then** $N_{\text{primitive}} \leftarrow N_{\text{primitive}} + 1$ **else** $N_{\text{operator}} \leftarrow N_{\text{operator}} + 1$ **end if****end while****end function**

stack operations (push, pop, top, indexing) can be achieved through the use of bitwise operators applied to the underlying integer. While a maximum stack size of 32 may seem limiting, we observed that for the ITER E-lite model (discussed at length in Section 3), which has a high degree of geometric complexity, the stack size was never greater than 9.

For prefix evaluation, rather than a stack of Boolean values, one needs to maintain a stack of operators. In this case, there are three possible values that need to be encoded: union, intersection, and a null value. Thus, each operator can be stored in 2 bits. By a similar argument, with a 32-bit unsigned integer one can carry out Algorithm 3 with as many as 16 operators on the stack at a given time. In our implementation in OpenMC, the stack stores the union operator as 01, the intersection operator as 10, and the null value as 00. An example of the memory layout of a stack containing four operators is shown in Fig. 4. In our tests using the ITER E-lite model, the operator stack never reached a size greater than 8 during point containment queries, confirming that a maximum stack size of 16 should be sufficient for nearly all use cases.

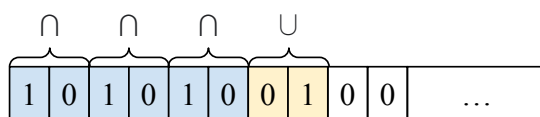


Figure 4: Example of bit-packing of 2-bit operators for a stack containing three set intersection operators followed by a single set union operator.

2.4. Infix Evaluation

Postfix and prefix notation have several advantages over infix notation, including the ability to enforce operator precedence without parentheses and straightforward evaluation algorithms, as demonstrated by Algorithm 1 and Algorithm 3. This is why several popular MC particle transport codes rely on postfix notation rather than infix. While we are aware of no codes that use prefix notation, the previous section showed that it can enable short-circuiting logic, which is not possible in postfix notation. However, we saw that with prefix notation it is necessary to manage a stack of 2-bit operators. While infix notation does not lend itself to as simple an evaluation algorithm as for postfix and prefix notations, we show here that it enables short-circuiting logic while requiring no stack data structure to manage during the evaluation of an expression.

Before presenting the algorithms for evaluating point containment using an infix notation, there is a peculiarity of the CSG representation in MC particle transport codes that must be considered. Namely, some codes (OpenMC, MCNP, and Serpent, for example) have an input representation wherein intersection operators are implicit; that is, the juxtaposition of two operands is interpreted as the intersection between the operands. With that representation, “ $-1 -2$ ” is the intersection of the negative half-spaces of two surfaces. This gives us two choices as to how to store the notation in memory and, correspondingly, how to evaluate point containment given the notation. If intersection operators are not stored in memory, we refer to the representation as being implicit; an example of this is shown in the left side of Fig. 5. If intersection operators *are* stored in memory, the representation is explicit (right side of Fig. 5).

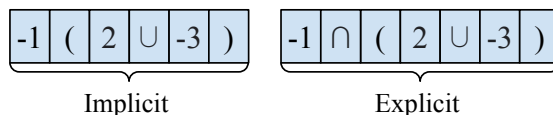


Figure 5: Memory representation (left-to-right) of the infix notation for the expression “ $-1 \cap (+2 \cup -3)$ ”.

Note that one important difference between the infix algorithms and the postfix/prefix algorithms is that the infix algorithm must keep track of parentheses, which now appear as tokens. For both infix evaluation algorithms, we assume that parentheses are always present to enforce precedence between operators, which may require

additional preprocessing at initialization. That is, if the user has provided an expression “ $-1 \cap 2 \cup -3$ ”, rather than internally relying on the assumed precedence of the \cup and \cap operators, a pair of parentheses is always inserted (e.g., “ $-1 \cap (2 \cup -3)$ ”).

The choice of an implicit or explicit memory representation has a direct impact on the corresponding evaluation algorithm. In the evaluation algorithm for an implicit representation, shown in Algorithm 5, the algorithm itself must deduce when an intersection operator is implied by the presence of two successive operands. Explicitly storing intersection operators in the memory representation simplifies the resulting algorithm. Algorithm 6 outlines the infix evaluation algorithm for an expression with intersection operators explicitly represented. We see that while an implicit representation minimizes memory use for the expressions, it does so at the expense of a more complex evaluation algorithm.

Both infix evaluation algorithms utilize short-circuiting that depends on the relative depth of parentheses as well as lazy evaluation of primitives. The short-circuiting algorithm, which simply skips ahead to the appropriate closing parenthesis in the notation, is given in Algorithm 7. Importantly, the use of short-circuiting logic is what allows the algorithm to keep track of only a single Boolean value rather than needing to store a stack of Boolean values. To understand this, note that the \vee operator is defined such that $x \vee y$ returns x if x is true and y otherwise. So, when x is true, the right operand does not need to be evaluated. When x is false, the result of the expression $x \vee y$ is y , meaning there is no need to store the value of x . A similar argument applies to $x \wedge y$; the expression short circuits when x is false and otherwise returns y , meaning the value of x needn't be stored.

3. Results

To measure the performance of the point containment evaluation algorithms based on postfix, prefix, and infix notations, all of them have been implemented on separate branches of the OpenMC particle transport code. Additionally, several variations on each algorithm were studied:

- **Postfix**—OpenMC version 0.13.1 [11] was used as the baseline for postfix notation. However, in this version, complement operators are present in the postfix notation, which therefore necessitates extra logic in the evaluation algorithm. A separate branch was created that uses De Morgan's laws to eliminate complements while otherwise preserving the postfix notation. Then, a third postfix branch that relies on a bit-packed stack allows us to study the impact of a more efficient stack data structure.
- **Prefix**—Two variations of the prefix evaluation algorithm were tested. First, a branch was created that implements the prefix evaluation algorithm and utilizes an operator stack based on the `std::vector` type. A second branch improves on this by utilizing a bit-packed operator stack.
- **Infix**—Two variations of the infix evaluation algorithm were tested: one that relies on an implicit memory representation and another that relies on an explicit memory representation.

Thus, there were seven different cases altogether that were tested, a summary of which is shown in Table 1. A code diff containing the changes to OpenMC for each of the cases is available in the data supplement to this article.

In OpenMC, CSG expressions are marked as either *simple* or *complex* at initialization. Simple expressions are defined to be those that involve only set intersection operators. For some CSG models, nearly all solids are represented with simple CSG expressions. Thus, OpenMC—and other codes—have separate evaluation logic for simple expressions as an optimization of the common case where it is straightforward to implement short-circuiting and lazy evaluation of primitives regardless of the notation being used. In order to test the efficacy of the algorithms presented here, then, we need a model that contains many solids with complex CSG expressions. For that, we rely on a detailed, realistic MCNP model of the ITER tokamak [14] called E-lite [12]. Whereas previous analysis models of the ITER tokamak only represented limited segments of the full machine [15], the E-lite model covers the full machine, thereby eliminating many previous modeling approximations. The E-lite model contains over 300,000 solids that are defined using over half a million implicit surfaces, making it—to our knowledge—one of the most complex radiation transport models in existence at the time of writing.

Algorithm 5 Infix surface half-space evaluation with implicit intersections. Note that it is assumed that parentheses have been inserted to enforce precedence.

Require: $T \equiv$ CSG expression in prefix notation

Require: $\mathbf{r} \equiv$ point in Euclidean space

function CONTAINSINFIXIMPLICIT(T, \mathbf{r})

$b \leftarrow$ TRUE

 ▷ Status variable

$d \leftarrow 0$

 ▷ Parentheses depth

$i \leftarrow 1$

 ▷ Index in T

while $i < \text{SIZE}(T)$ **do**

$x \leftarrow T[i]$

 ▷ Get next node

if x is a primitive **then**

if $b = \text{TRUE}$ **then**

$b \leftarrow \text{EVALUATE}(x, \mathbf{r})$

else if $d = 0$ **then**

break

end if

else if x is \cup **then**

if $b = \text{FALSE}$ **then**

$b \leftarrow \text{TRUE}$

 ▷ Reset return status

else if d is 0 **then**

break

else

$d \leftarrow d - 1$

 SHORTCIRCUITINFIX(T, i)

end if

else if x is (**then**

if $b = \text{FALSE}$ **then**

 SHORTCIRCUITINFIX(T, i)

else

$d \leftarrow d + 1$

end if

else if x is) **then**

$d \leftarrow d - 1$

end if

end while

return b

end function

Algorithm 6 Infix surface half-space evaluation with explicit intersections

Require: $T \equiv$ CSG expression in prefix notation

Require: $\mathbf{r} \equiv$ point in Euclidean space

function CONTAINSINFIX(T, \mathbf{r})

$b \leftarrow \text{TRUE}$

▷ Boolean value to be returned

$d \leftarrow 0$

▷ Parentheses depth

$i \leftarrow 1$

▷ Index in T

while $i < \text{SIZE}(T)$ **do**

$x \leftarrow T[i]$

▷ Get next node

if x is a primitive **then**

$b \leftarrow \text{EVALUATE}(x, \mathbf{r})$

else if (x is \cup and $b = \text{TRUE}$) or (x is \cap and $b = \text{FALSE}$) **then**

if $d = 0$ **then**

break

else

$d \leftarrow d - 1$

SHORTCIRCUITINFIX(T, i)

end if

else if x is (**then**

$d \leftarrow d + 1$

else if x is) **then**

$d \leftarrow d - 1$

end if

end while

return b

end function

Algorithm 7 Short-circuiting algorithm used by both infix algorithms

Require: $T \equiv$ CSG expression in prefix notation

Require: $i \equiv$ Index in T

function SHORTCIRCUITINFIX(T, i)

$d' \leftarrow 1$

while $d' > 0$ **do**

▷ Loop until end of parentheses

$i \leftarrow i + 1$

$x \leftarrow T[i]$

▷ Get next node

if x is (**then**

$d' \leftarrow d' + 1$

else if x is) **then**

$d' \leftarrow d' - 1$

end if

end while

end function

Table 1: Summary of OpenMC branches implementing different point containment algorithms.

Algorithm	Complement expanded?	Bit-packed stack?	Implicit intersection?
Postfix-1			—
Postfix-2	✓		—
Postfix-3	✓	✓	—
Prefix-1	✓		—
Prefix-2	✓	✓	—
Infix-1	✓	—	✓
Infix-2	✓	—	

In order to use the E-lite MCNP model with OpenMC, it was converted using an automated MCNP model conversion utility [16]. Figures 6 and 7 show horizontal and vertical cross-sectional views of the resulting OpenMC model that were generated using OpenMC’s built-in visualization capabilities. The model conversion utility seamlessly handles conversion of implicit surfaces, solid bodies, and the material composition definitions that are assigned to solid bodies. Some aspects of the model are not handled, however, including the definition of the neutron source, which is needed in order to carry out a neutron transport simulation. For the OpenMC model, the neutron source definition was manually specified as the superposition of 40 individual sources in (r, ϕ, z) to approximate the original source definition in the MCNP model.

From here, we present our results in three parts. First, in Section 3.1, we present performance results for the generation of a 2D slice visualization of the E-lite model based on rasterization using each of the algorithms in Table 1. Then, in Section 3.2, performance results are given for neutron transport simulations of E-lite using each algorithm in Table 1. Finally in Section 3.3, we show performance profiles of OpenMC simulations of the E-lite model utilizing each algorithm to better understand where performance improvements arise for the prefix and infix notations.

3.1. Rasterization Performance

To isolate the performance impact of the point containment algorithms as much as possible, our first integrated test is based on a function in OpenMC that performs rasterization to produce a 2D slice visualization, such as those shown in Figs. 6 and 7. The function iterates over a set of Cartesian points in a given plane and, for each one, performs a search to determine what solid body the point is contained in. For each point, the search proceeds by iterating over all top-level solid bodies and performing a point containment search on its associated CSG expression until one is found that contains the point. Because nearly all the execution time is spent in point containment searches, this function allows us to measure the performance impact of the different algorithms without being diluted by other transport operations.

Each of the branches listed in Table 1 was used to produce a single high-resolution 2D slice visualization with 3600×3600 pixels with a call to the `openmc_id_map` C API function. Three iterations were performed for each branch and we took the lowest time for each branch. The runs were carried out on the Bebop cluster maintained by the Laboratory Computing Resource Center at Argonne National Laboratory. Each test was run on one Intel Xeon E5-2695v4 processor with 18 cores. The timing results are presented in Table 2. The baseline version of OpenMC (Postfix-1) took 12.36 s to generate the rasterized image. Interestingly, expanding complement operators (Postfix-2) appears to slightly worsen the performance. However, the use of a bit-packed stack for Boolean values results in a 50% improvement over the baseline. Adopting a prefix notation (Prefix-1), which allows the evaluation algorithm to benefit from short-circuiting, performs even better with an execution time 2.3 times faster than the baseline. Improving the data structure for the operator stack (Prefix-2) improves the performance even more, resulting in a $3 \times$ speedup over the baseline. Finally, the infix evaluation algorithms perform the best of all, with improvements of $5.29 \times$ (implicit) and $6.11 \times$ (explicit) relative to the baseline.

Table 2: Timing results for producing a high-resolution raster plot using OpenMC with each point containment algorithm. Performance improvement is measured relative to Postfix-1.

Algorithm	Time [s]	Performance improvement
Postfix-1	12.36	1.00
Postfix-2	12.61	0.98
Postfix-3	8.32	1.49
Prefix-1	5.38	2.30
Prefix-2	4.17	2.97
Infix-1	2.34	5.29
Infix-2	2.02	6.11

3.2. Transport Performance

The results in Section 3.1 show that using prefix or infix notation results in significant performance improvements for point containment operations relative to postfix notation. To demonstrate the impact in an actual neutron transport simulation, we have carried out full simulations of the E-lite OpenMC model using each algorithm from Table 1. Once again, all simulations were run on one node of the Bebop cluster containing two Intel Xeon E5-2695v4 processors. Each OpenMC simulation used two MPI processes, 18 OpenMP threads per process, 10,000 source particles per batch, and 10 total batches. OpenMC reports the calculation throughput in terms of source particles simulated per second. For each algorithm, we ran three simulations and took the best result². The performance results for the transport simulations are shown in Table 3. The results follow the same trends as in Table 2 with a few exceptions. In this case, Postfix-2 performs slightly better than Postfix-1, where for rasterization it performed slightly worse. For the transport simulation results, it is expected that the overall performance improvement would be slightly less than for rasterization since the simulation involves many other operations. Nevertheless, utilization of point containment algorithms based on prefix and infix notation offer up to 2.50 \times and 4.59 \times performance improvement, respectively, for the *entire* transport simulation of the E-lite model. The impressive performance results here led to the inclusion of the algorithm based on infix notation with an explicit memory representation in version 0.13.2 of OpenMC [17].

Table 3: Measured simulation throughput in source particles per second for neutron transport simulations of the E-lite model using OpenMC with each point containment algorithm. Performance improvement is measured relative to Postfix-1.

Algorithm	Rate [particles/s]	Performance improvement
Postfix-1	180.9	1.00
Postfix-2	187.3	1.04
Postfix-3	251.1	1.39
Prefix-1	328.0	1.81
Prefix-2	452.8	2.50
Infix-1	740.6	4.09
Infix-2	830.4	4.59

²We note that the results across the three independent runs were very consistent in all cases, with less than 1% difference in the measured throughput.

3.3. Performance Profiles

During a particle transport simulation, many different operations must be carried out including collision physics, geometry lookups, cross-section (interaction probability) lookups, and tallies. To provide further context to the results in Section 3.2, we have utilized `perf` (also known as `perf_events`), a Linux performance analysis tool, to profile the execution of several short simulation (10 batches, each with 1000 particles) of the E-lite model using algorithms Postfix-1, Prefix-2, and Infix-2. Each branch of OpenMC was compiled with the CMake option `OPENMC_ENABLE_PROFILE` turned on³. Neutron cross sections from ENDF/B-VIII.0 [18] were used in the simulation. The simulations were run on a laptop with an Intel Core i7-1260P processor and used only one OpenMP thread. Figure 8 shows the time spent in the most expensive functions for each algorithm. The four functions that are specifically called out are as follows:

1. `CSGCell::contains_complex` — This function handles the evaluation logic for point containment on a complex CSG expression (Algorithm 1, Algorithm 3, or Algorithm 6).
2. `Surface::sense` — This function evaluates an implicit surface inequality as in Algorithm 2.
3. `SurfacePlane::evaluate` — This function is called by `Surface::sense` when it needs to evaluate the implicit surface equation for a plane.
4. `SurfaceQuadric::evaluate` — This function is called by `Surface::sense` when it needs to evaluate the implicit surface equation for a generic quadric (e.g., an ellipsoid or elliptic paraboloid).

Several observations can be made on the results in Fig. 8. First, we see that the use of prefix and infix notation significantly reduces the time spent evaluating the CSG binary tree expressions (blue). In addition, the time spent evaluating point containment on primitives (orange, green, and red) are also reduced significantly thanks to the use of short-circuiting logic. Lastly, the time spent in all other functions (purple) is also slightly reduced as it also includes a number of functions that are called fewer times due to short-circuiting.

4. Conclusions

In this article, we have presented several algorithms for evaluating point containment in CSG trees with unbounded primitives. While the algorithms are not specific to the representative of the primitives, we have drawn on examples from Monte Carlo particle transport simulations, which often use CSG trees based on implicit surface inequalities. Three basic algorithms were presented, each based on a different notation of the CSG expression: postfix, prefix, and infix. It was shown that prefix and infix allow short-circuiting logic to be used, which reduces the number of primitives that must be checked during point containment. Furthermore, we discussed storage requirements for intermediate results during the execution of point containment algorithms. Both postfix and prefix notation necessitate the use of a stack during evaluation, whereas infix notation eliminates the need for a stack altogether. Techniques for minimizing memory use and, correspondingly, dynamic memory allocation for the stack were discussed for evaluations using the postfix and prefix notations.

To evaluate the performance of the various algorithms, two sets of tests were carried out using the OpenMC Monte Carlo code along with several modified branches of it. First, the execution time to generate a high-resolution rasterized image of a 2D slice of a detailed CSG model of the ITER tokamak was measured with each of the various algorithms. Use of both prefix and infix notations offered significant speedup over the postfix notation that has traditionally been used in MC particle transport codes, with infix resulting in a 6× reduction in execution time for image generation relative to postfix. For postfix and prefix notations, which require a stack of intermediate results, the use of a bit-packed stack led to roughly 40% improvement in performance over the use of a traditional C++ data structure like `std::vector`. Finally, for infix notation, we looked at the difference between explicitly representing set intersection operators in the notation versus representing them implicitly; the result demonstrates that the explicit representation outperforms the implicit representation due to simplifications in the algorithm.

³This option ensures that the gcc compiler uses the `-fno-omit-frame-pointer` flag which is necessary for producing accurate profiles.

In addition to the rasterization tests, we also measured the execution time of neutron transport simulations of the ITER E-lite model using each of the various algorithms. The results and performance improvements reveal the same trends as for rasterization, although the addition of other operations in the transport loop means that the performance improvements are slightly less—in this case, a $4.59\times$ overall speedup using the infix notation relative to the baseline postfix notation.

While the results that we have reported here are specifically for CPU architectures, we expect that the performance gains will translate to other architectures as well. Anecdotally, we have observed similar performance gains for fusion-relevant problems with the use of infix notation on GPUs within a GPU port of OpenMC based on OpenMP device offloading [19].

It is important to recognize that the improvements demonstrated for the ITER E-lite model are not representative of all MC transport simulations. As noted, many MC codes are already optimized for CSG expressions involving only set intersection operators. Many CSG models for particle transport simulations have a high fraction of solids that can be represented with such expressions, and thus we would not expect to realize any performance benefit for these models. However, for geometrically complex models, which occur quite commonly for fusion energy—and possibly other—applications, significant performance benefit can be expected from the algorithmic advancements presented herein.

The scope of this paper has been limited solely to a single operation—evaluating point containment on a CSG tree. Of course, there are many other techniques one can use to accelerate spatial searches. In Section 3.1, we described how the search for the solid body containing a given point in OpenMC involves a linear search over all top-level solid bodies in the model. Use of a bounding volume hierarchy or other spatial acceleration data structure / algorithm can also greatly reduce the time needed to perform these spatial searches. Other techniques to simplify and/or reorder the operations in the CSG binary expression tree could similarly improve performance.

Data Availability

The data that support the findings of this study are openly available at the following DOI: [10.5281/zenodo.10045317](https://doi.org/10.5281/zenodo.10045317).

CRediT Author Statement

Paul K. Romano: Conceptualization, Investigation, Visualization, Writing — Original Draft, Writing — Review & Editing, Supervision, Project administration, Funding acquisition. **Patrick A. Myers:** Methodology, Software, Investigation, Writing — Original Draft. **Seth R. Johnson:** Software, Writing — Review & Editing. **Aljaž Kolšek:** Software, Writing — Review & Editing. **Patrick C. Shriwise:** Conceptualization, Writing — Review & Editing.

Acknowledgments

This work is supported by the U.S. Department of Energy Office of Fusion Energy Sciences under award number DE-SC0022033. We gratefully acknowledge the computing resources provided on Bebop, a high-performance computing cluster operated by the Laboratory Computing Resource Center at Argonne National Laboratory. This work was carried out using an adaption of the E-lite model which was developed as a collaborative effort between: AMEC Co (International), CCFE (UK), ENEA Frascati (Italy), FDS Team of INEST (PRC), ITER Organization (France), QST (Japan), KIT (Germany), UNED (Spain), University of Wisconsin-Madison (USA), F4E (Europe). The views and opinions expressed herein do not necessarily reflect those of the ITER Organization.

References

- [1] A. A. G. Requicha, H. B. Voelcker, Constructive solid geometry, Tech. Rep. TM-25, The University of Rochester, Rochester, NY (Nov. 1977).
- [2] J. D. Foley, A. van Dam, S. K. Feiner, J. F. Hughes, Computer Graphics: Principles and Practice, 2nd Edition, Addison-Wesley Publishing Company, 1990.
- [3] A. G. Requicha, Representations for rigid solids: Theory, methods, and systems, ACM Comput. Surv. 12 (4) (1980) 437–464. doi: 10.1145/356827.356833.

- [4] A. A. G. Requicha, H. B. Voelcker, Boolean operations in solid modeling: Boundary evaluation and merging algorithms, *Proc. IEEE* 73 (1985) 30–44. doi:10.1109/PROC.1985.13108.
- [5] P. K. Romano, N. E. Horelik, B. R. Herman, A. G. Nelson, B. Forget, OpenMC: A state-of-the-art Monte Carlo code for research and development, *Ann. Nucl. Energy* 82 (2015) 90–97. doi:10.1016/j.anucene.2014.07.048.
- [6] J. A. Kulesza, T. R. Adams, J. C. Armstrong, S. R. Bolding, F. B. Brown, J. S. Bull, T. P. Burke, A. R. Clark, R. A. Forster III, J. F. Giron, T. S. Grieve, C. J. Josey, R. L. Martz, G. W. McKinney, E. J. Pearson, M. E. Rising, C. J. Solomon Jr., S. Swaminarayan, T. J. Trahan, S. C. Wilson, A. J. Zukaitis, MCNP code version 6.3.0 theory & user manual, Tech. Rep. LA-UR-22-30006, Los Alamos National Laboratory, Los Alamos, New Mexico (Sep. 2022). doi:10.2172/1889957.
- [7] T. M. Pandya, S. R. Johnson, T. M. Evans, G. G. Davidson, S. P. Hamilton, A. T. Godfrey, Implementation, capabilities, and benchmarking of Shift, a massively parallel Monte Carlo radiation transport code, *J. Comput. Phys.* 308 (2016) 239–272. doi:10.1016/j.jcp.2015.12.037.
- [8] T. Böhlen, F. Cerutti, M. Chin, A. Fassò, A. Ferrari, P. Ortega, A. Mairani, P. Sala, G. Smirnov, V. Vlachoudis, The FLUKA code: Developments and challenges for high energy and medical applications, *Nuclear Data Sheets* 120 (2014) 211–214. doi:10.1016/j.nds.2014.07.049.
- [9] J. Leppänen, M. Pusa, T. Viitanen, V. Valtavirta, T. Kaltiaisenaho, The Serpent Monte Carlo code: Status, development, and applications in 2013, *Ann. Nucl. Energy* 82 (2015) 142–150. doi:10.1016/j.anucene.2014.08.024.
- [10] F. W. Jansen, Depth-order point classification techniques for CSG display algorithms, *ACM Trans. Graph.* 10 (1) (1991) 40–70. doi:10.1145/99902.99904.
- [11] P. K. Romano, et al., OpenMC 0.13.1, <https://doi.org/10.5281/zenodo.7010045> (Aug. 2022).
- [12] R. Juarez, G. Pedroche, M. J. Loughlin, R. Pampin, P. Martinez, M. D. Pietri, J. Alguacil, F. Ogando, P. Sauvan, A. J. Lopez-Revelles, A. Kolšek, E. Polunovskiy, M. Fabbri, J. Sanz, A full and heterogeneous model of the ITER tokamak for comprehensive nuclear analyses, *Nat. Energy* 6 (2021) 150–157. doi:10.1038/s41560-020-00753-x.
- [13] E. W. Dijkstra, Algol 60 translation: An algol 60 translator for the x1 and making a translator for algol 60, Tech. Rep. MR 34/61, Stichting Mathematisch Centrum, Amsterdam, Netherlands (1961).
URL <https://www.cs.utexas.edu/users/EWD/MCReps/MR35.PDF>
- [14] N. Holtkamp, ITER Project Team, et al., An overview of the ITER project, *Fusion Eng. Des.* 82 (5–14) (2007) 427–434. doi:10.1016/j.fusengdes.2007.03.029.
- [15] D. Leichtle, B. Colling, M. Fabbri, R. Juarez, M. Loughlin, R. Pampin, E. Polunovskiy, A. Serikov, A. Turner, L. Bertalot, The ITER tokamak neutronics reference model C-Model, *Fusion Eng. Des.* 136 (2018) 742–746. doi:10.1016/j.fusengdes.2018.04.002.
- [16] Paul K. Romano and Stefano Segantin, MCNP Conversion Tools for OpenMC, https://github.com/openmc-dev/openmc_mcnp_adapter (Oct. 2023).
- [17] P. K. Romano, et al., OpenMC 0.13.2, <https://doi.org/10.5281/zenodo.7236328> (Oct. 2022).
- [18] D. A. Brown, M. B. Chadwick, R. Capote, A. C. Kahler, A. Trkov, M. W. Herman, A. A. Sonzogni, Y. Danon, A. D. Carlson, M. Dunn, D. L. Smith, G. M. Hale, G. Arbanas, R. Arcilla, C. R. Bates, B. Breck, B. Becker, F. Brown, R. J. Casperson, J. Conlin, D. E. Cullen, M.-A. Descalle, R. Firestone, T. Gaines, K. H. Guber, A. I. Hawari, J. Holmes, T. D. Johnson, T. Kawano, B. C. Kiedrowski, A. J. Koning, S. Kopecky, L. Leal, J. P. Lestone, C. Lubitz, J. I. Márquez Damián, C. M. Mattoon, E. A. McCutchan, S. Mughabghab, P. Navratil, D. Neudecker, G. P. A. Nobre, G. Noguere, M. Paris, M. T. Pigni, A. J. Plompen, B. Pritychenko, V. G. Pronyaev, D. Roubtsov, D. Rochman, P. Romano, P. Schillebeeckx, S. Simakov, M. Sin, I. Sirakov, B. Sleaford, V. Sobes, E. S. Soukhovitskii, I. Stetcu, P. Talou, I. Thompson, S. van der Marck, L. Welsch-Sherrill, D. Wiarda, M. White, J. L. Wormald, R. Q. Wright, M. Zerke, G. Žerovnik, Y. Zhu, ENDF/B-VIII.0: The 8th major release of the nuclear reaction data library with CIELO-project cross sections, new standards and thermal scattering data, *Nucl. Data Sheets* 148 (2018) 1–142. doi:10.1016/j.nds.2018.02.001.
- [19] John R. Tramm and others, GPU port of the OpenMC Monte Carlo code, <https://github.com/exasmr/openmc> (Oct. 2023).

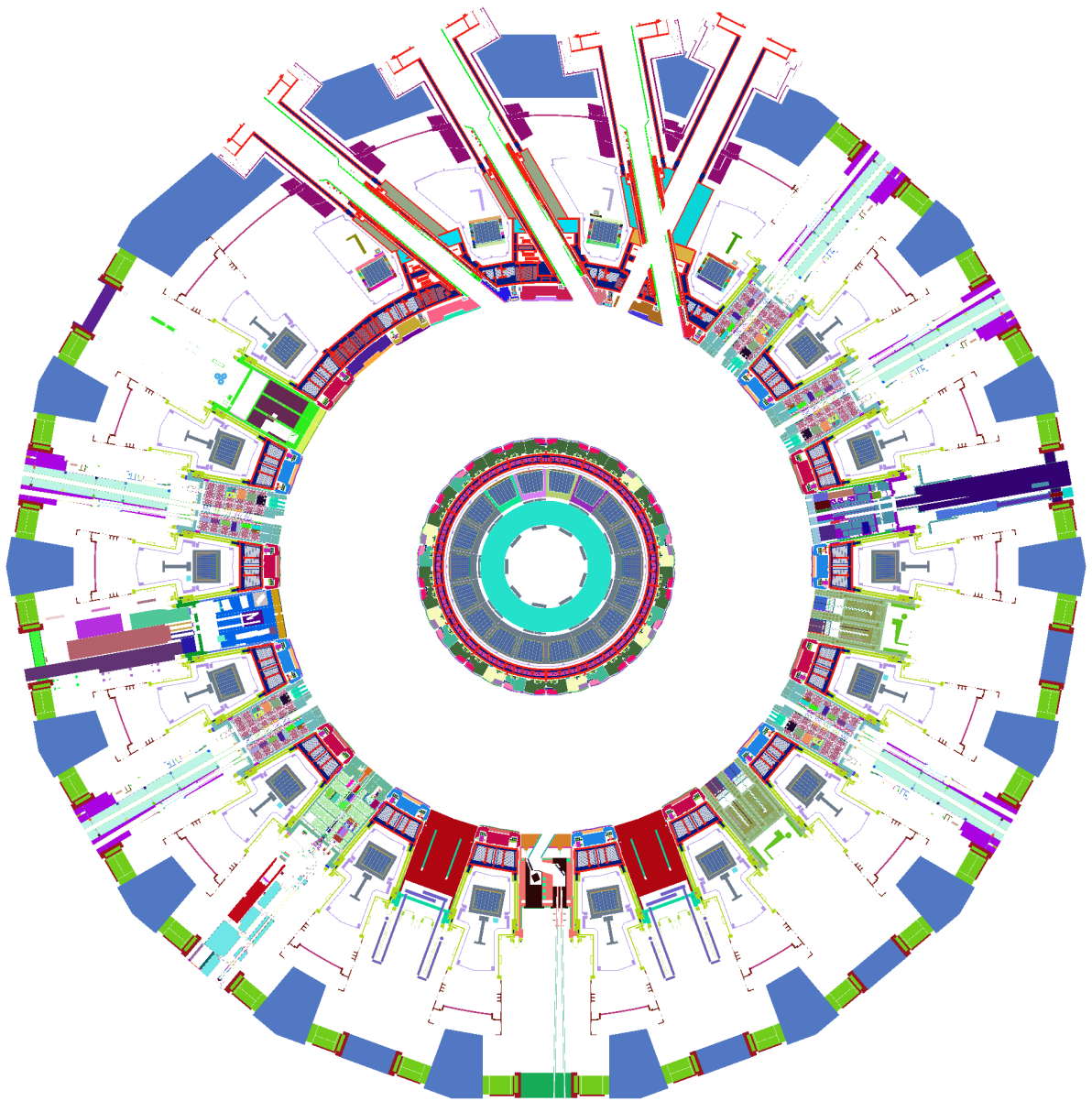


Figure 6: Horizontal (x-y) cross-sectional view of the ITER E-lite OpenMC model at an elevation of $z=60$ cm.

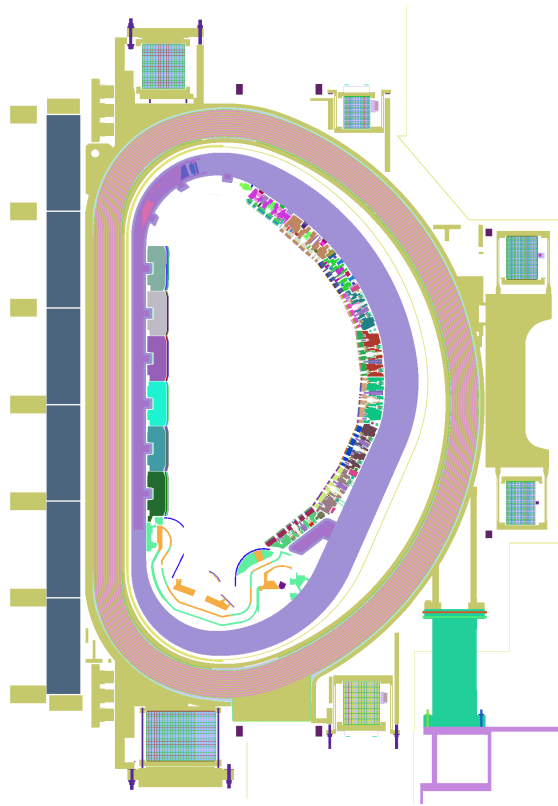


Figure 7: Vertical (x - z) cross-sectional view of the ITER E-lite OpenMC model.

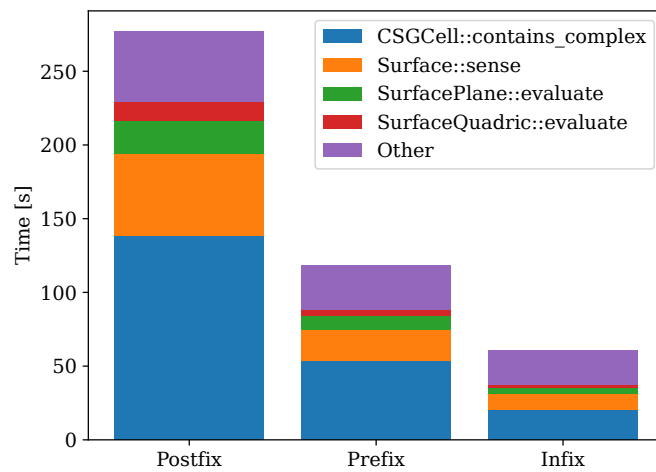


Figure 8: Time spent in selected functions during OpenMC execution of a neutron transport simulation of the ITER E-lite model based on each evaluation algorithm.

The submitted manuscript has been created by UChicago Argonne, LLC, Operator of Argonne National Laboratory (“Argonne”). Argonne, a U.S. Department of Energy Office of Science laboratory, is operated under Contract No. DE-AC02-06CH11357. The U.S. Government retains for itself, and others acting on its behalf, a paid-up nonexclusive, irrevocable worldwide license in said article to reproduce, prepare derivative works, distribute copies to the public, and perform publicly and display publicly, by or on behalf of the Government. The Department of Energy will provide public access to these results of federally sponsored research in accordance with the DOE Public Access Plan. <https://energy.gov/downloads/doe-public-access-plan>